Ceramics International xxx (xxxx) xxx–xxx

Contents lists available at ScienceDirect

Ceramics International

journal homepage: www.elsevier.com/locate/ceramint

Synthesis and characterization of reaction-bonded calcium alumino-titanate-bauxite-SiC composite refractories in a reducing atmosphere

Jianwei Chen[a], Huizhong Zhao[a], Jun Yu[a], Han Zhang[a,*], Zhengkun Li[b], Jiaqin Zhang[b]

[a] The State Key Laboratory of Refractory and Metallurgy, Wuhan University of Science and Technology, Wuhan 430081, China
[b] Jiangsu Jingxin New Materials Co., Ltd., Yangzhou 225265, China

ARTICLE INFO

Keywords:
CAT-bauxite-SiC
Low melting phase
Buried sintering
High-temperature performance
Alkali resistance

ABSTRACT

To take full advantage of the excellent properties of CA_6 present in calcium alumino-titanate (CAT) and reduce the formation of the low melting point phase (anorthite), CAT-bauxite-SiC composite refractories were fabricated under buried sintering in order to achieve low thermal expansion, superior high-temperature performance, and increased alkali resistance. Furthermore, the corrosion mechanism of K vapor was investigated by means of X-ray diffraction (XRD) and scanning electron microscopy (SEM). Results show that CA_6 present in CAT can be partially retained and the hot strength of CAT-bauxite-SiC composites slowly decreases when the amount of CAT added is less than 21.6 wt%. The cold strength and bulk density decrease with the CAT content, and the residual ratio of MOR firstly decreases and subsequently increases with the CAT content. For the specimens with CAT additions, 43.2 wt% CAT results in the highest volume expansion at high temperatures. It is proposed that the corrosion mechanism of CAT aggregates under buried sintering is as follows: 1) K vapors penetrate into the CAT with high CA_6 content through the lamellar CA_6 gap and deposit on the inner regions of CAT; and 2) K vapors react with corundum and anorthite present in CAT and cause the microstructural destruction of CAT due to a decrease in the amount of the Al_2O_3-CaO-SiO_2 liquid phase in the CAT. The alkali resistance of the CAT-bauxite-SiC composites decreases as the CAT content increases, which is attributed to poor sintering densification and high apparent porosity.

1. Introduction

The treatment of alloy smelting waste has been extensively investigated in the last few decades [1–5], including separation, purification, and direct replacement applications. Samal et al. [6] converted feed ilmenite into synthetic rutile in a two-step process, consisting of plasma melt separation and leaching. Furthermore, Samal et al. also investigated the relevant criteria for titania slag leaching in hydrochloric acid, including the acid concentration, experimental parameters and solid/liquid ratio [7], and the application of thermal plasma technology in waste materials, coating, spraying, ilmenite, and other similar materials and process [8,9]. Qi Tao et al. [10] proposed an anti-cracking method for the decomposition of low-grade titanium slag in the NaOH system in a two-step molten salt reaction at different temperatures. Langmesser et al. [11] and Mackey et al. [12] proposed commercial technologies for the manufacture of pigment-grade titanium dioxide by the sulfate process, in which ilmenite is digested with strong sulfuric acid, yielding a titanium sulfate solution which is then hydrolyzed and precipitated to form a TiO_2 pigment. Furthermore, the calcium alumino-titanate (CAT) addition can improve the slag-resistant properties of high aluminum bauxite castable, because CAT easily reacts with slag and increases its viscosity [13].

CAT raw materials have good properties [14–16], such as low coefficients of thermal expansion and thermal conductivity, high-melting point, and high refractoriness, due to its multiphase system that includes CA_6, $Ca((Al_{0.84}Ti_{0.16})_2)_6O_{19}$, CA_2, and $CaTiO_3$ [17–19]. Furthermore, when CAT is heated, the phases present in CAT raw materials change and the CA_6 content accounts for about 70 wt% [15]. In view of the excellent properties of CA_6 [20–22], applying CAT raw materials significantly improves the part performance of composite refractories.

However, in our previous study, CAT-bauxite-SiC composites fired in an oxidizing atmosphere exhibited poor high-temperature performance of the hot strength and refractoriness under load [14]. CA_6 and CA_2 phases present in CAT in bauxite-SiC composites at high temperatures undergo the following transformation: 1) CA_2 reacts with corundum to form CA_6, with an accompanying volume expansion; 2) CA_6 reacts with SiO_2, oxidized by metallic Si and SiC, to form anorthite, causing the calcium ions to diffuse out from the hexagonal system.

* Corresponding author.
E-mail address: wustzh@163.com (H. Zhang).

https://doi.org/10.1016/j.ceramint.2018.05.183
Received 18 March 2018; Received in revised form 15 May 2018; Accepted 21 May 2018

Furthermore, the oxidization of metallic Ti and Fe present in CAT results in volume expansion. Therefore, decreasing the content of anorthite and liquid phase, avoiding the over-oxidization of SiC, fixing calcium ions in the hexagonal system, and retaining the lamellar structure of CA_6, are critical factors for improving the high-temperature performance of CAT-bauxite-SiC composites.

Thus, the present work is intended to determine the feasibility of obtaining CAT-bauxite-SiC composites by firing at 1450 °C in a reducing atmosphere to enhance the service performance of CAT-bauxite-SiC composites.

2. Experimental

2.1. Specimen preparation

High-grade bauxite (3–1 mm, 1–0 mm, and < 0.088 mm; 85.5 wt% Al_2O_3, 8.61 wt% SiO_2, 1.25 wt% Fe_2O_3, and 3.33 wt% TiO_2), CAT (3–1 mm, 1–0 mm, < 0.088 mm, and < 0.058 mm; 74.18 wt% Al_2O_3, 11.69 wt% CaO, and 11.08 wt% TiO_2), SiC (< 0.088 mm; 98.72 wt% SiC), α-alumina (< 0.088 mm; 99.06 wt% Al_2O_3), Guang Xi white clay (< 0.088 mm; 33.03 wt% Al_2O_3 and 49.25 wt% SiO_2), and metallic silicon powder (< 0.088 mm; 98.9 wt% Si) were used as raw materials. Commercially available $Al(H_2PO_4)_3$ solution (liquid, specific gravity of 1.40) was used as a binder. The specimens were mixed for 8–10 min and then pressed into bar-shaped specimens with dimensions of 25 × 25 × 156 mm^3 (to be used for mechanical property and thermal shock resistance tests) and cylindrical specimens with dimensions of Φ50 × 50 mm^3 (to be used for refractoriness under load and thermal expansion tests) at a pressure of 170 MPa. After drying at 110 °C for 24 h, the specimens were fired at 1450 °C for 3 h in a coke bed. The prepared specimens are listed in Table 1.

2.2. Characterization

Modulus of rupture (MOR) was measured by three-point bending tests at room temperature with a span of 80 mm and a loading rate of 0.5 mm/min. The hot modulus of rupture (HMOR) was determined by performing three-point tests using a 125-mm span at 1400 °C. The bulk density and apparent porosity were measured using the Archimedes method. The linear change ratio, cold crushing strength (CCS), and refractoriness under load (RUL) were measured according to GB/T 5988-2007, GB/T 5072-2008, and GB/T 5989-2008, respectively. The fired specimens were heated from room temperature (20 °C) to 1100 °C at a heating rate of 5 °C/min for a holding time of 30 min, followed by fast quenching in compressed air at room temperature for 5 min. Then, the residual ratio of MOR after three thermal cycles were measured. The coefficient of thermal expansion (CTE) was measured under a constant load at a heating rate of 5 °C/min from room temperature to 1400 °C.

The alkali resistance test was performed using specimens previously fired at 1450 °C with dimensions of Φ50 × 30 mm^3 that were embedded in premixed potassium carbonate and carbon black (1:1 wt%) powders in graphite crucibles. The graphite crucibles were placed in an alumina crucible and surrounded by carbon powder and fired at 1000 °C for 10 h. Phase analysis of the specimens before and after alkali treatment was performed by X-ray diffraction (XRD; X'Pert Pro, Philips), with Ni-filtered, Cu K_α radiation at a scanning speed of 2°/min at 20 °C. The microstructural evolution in the specimens before and after alkali attack was examined by scanning electron microscopy (SEM; Nova400 Nano SEM, FEI Company, USA) and elemental analysis was performed by energy dispersive X-ray spectroscopy (EDS, Phoenix EDS Microanalysis system, EDAX, Inc., USA).

Table 1
Compositions of the specimens.

Specimen no.		Ref	CBT20	CBT40	CBT60	CBT80	CBT100
Bauxite	3–1	40	32	24	16	8	0
	1–0	14	11.2	8.4	5.6	2.8	0
	< 0.088	24.5	24.5	24.5	24.5	24.5	24.5
CAT	3–1	0	8	16	24	32	40
	1–0	0	2.8	5.6	8.4	11.2	14
SiC	1–0	8	8	8	8	8	8
	< 0.088	5	5	5	5	5	5
Guang Xi white clay	< 0.088	4	4	4	4	4	4
Si	< 0.088	1.5	1.5	1.5	1.5	1.5	1.5
α-Al_2O_3	< 0.088	3	3	3	3	3	3
$Al(H_2PO_4)_3$		+ 3	+ 3	+ 3	+ 3	+ 3	+ 3

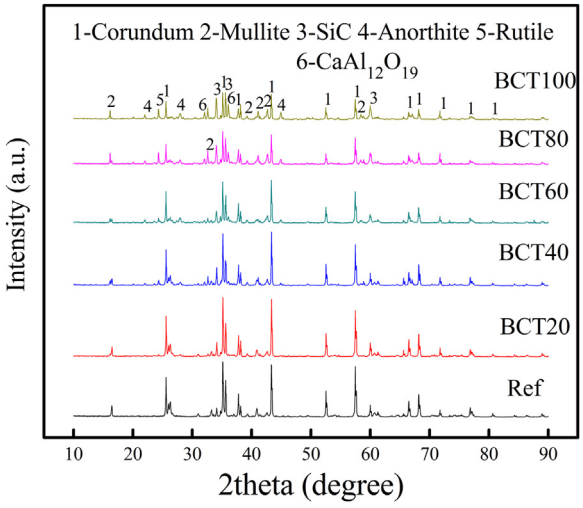

Fig. 1. XRD patterns of the specimens before alkali attack.

3. Results

3.1. Phase and microstructure analysis

The XRD patterns of the specimens before alkali attack are shown in Fig. 1. The main crystalline phases of all the specimens are corundum, mullite, and SiC. Furthermore, CA_6, anorthite, and rutile phases are detected when the CAT is added. The intensities of the corundum diffraction peaks decrease with the CAT content; however, the intensities of the anorthite, rutile, and mullite diffraction peaks increase with the CAT content. The formation of rutile and anorthite can be attributed to the desolvation of $Ca((Al_{0.84}Ti_{0.16})_2)_6O_{19}$ and the reactions between CA_2, CA_6, and SiO_2, respectively [14].

The SEM images of specimen BCT40 are shown in Fig. 2. Some mullite and SiC whiskers are observed, which is attributed to the formation of SiO vapor. According to the study by Lian et al. [23], the mullite and SiC whiskers are formed by the VLS growth mechanism. Under buried sintering, SiO and CO vapors are produced, and then react with each other to form SiC that is deposited on the surface of the bauxite/CAT/SiC aggregates. Furthermore, lamellar CA_6 grains are observed in the CAT aggregates (Fig. 3), showing different aggregation states, such as embedded, cross, and stacked types. The appearance of CA_6 phase indicates that the reducing atmosphere slows the diffusion of Ca ions to the edge of bauxite/SiC aggregates to a certain extent.

3.2. Mechanical properties

The physical properties (linear change ratio, bulk density, apparent porosity, MOR, CCS, HMOR, and RUL) of all the specimens are shown in Table 2. The linear change ratio and apparent porosity of the specimens increase with CAT content; however, the bulk density, MOR, CCS, HMOR, and RUL decrease with increased CAT content. According to the